Single-photon source characterization with twin infrared-sensitive superconducting single-photon detectors

Robert H. Hadfield,[a] Martin J. Stevens, Richard P. Mirin, and Sae Woo Nam
National Institute of Standards and Technology, 325 Broadway, Boulder, Colorado 80305

(Received 27 November 2006; accepted 9 February 2007; published online 21 May 2007)

We report on the high fidelity characterization, via spontaneous emission lifetime and $g^{(2)}(\tau)$ measurements, of a cavity-coupled quantum dot single-photon source at 902 nm using a pair of nanowire-based superconducting single-photon detectors (SSPDs). We analyze the suitability of the twin SSPD scheme reported here for the characterization of single-photon sources at telecommunications wavelengths (1310 and 1550 nm). © *2007 American Institute of Physics*.
[DOI: 10.1063/1.2717582]

I. INTRODUCTION

Quantum information processing promises to revolutionize the fields of communications[1,2] and computing[3] over the coming decades. Applications in this burgeoning area hinge upon the ability to produce and detect single photons. Practical quantum communication systems will likely take advantage of the existing telecommunications fiber optic infrastructure, which operates in wavelength bands around 1310 and 1550 nm. Thus, the development of more efficient single-photon sources and detectors in the telecommunications wavelength bands is critical to the implementation of quantum information technologies in the real world.

Quantum dot single-photon sources were initially demonstrated with emission at wavelengths shorter than 1 μm.[4,5] Although progress has been made in the development of quantum dot single-photon sources emitting near 1300 nm,[6,7] characterization of these sources has been difficult, owing to the scarcity of good single-photon detectors in this wavelength range. Silicon avalanche photodiodes (APDs), which are the detectors of choice for visible-light photon counting,[8] are insensitive to wavelengths beyond ~1050 nm. For single-photon counting at longer wavelengths, InGaAs APDs are employed.[9] These detectors have detection efficiencies (η) up to 50% and are typically limited to clock rates of ~1 MHz in order to avoid afterpulsing. Also, gating is essential to reduce the very high dark count rates (up to ~100 kHz ungated).

Nanowire-based superconducting single-photon detectors (SSPDs) hold great promise for visible and infrared single-photon counting applications. These devices[10–13] have intrinsic η up to 20% in the visible with very few dark counts. They are extremely fast (the minimum reported jitter is 20 ps) and can be clocked at very high rates (up to ~1 GHz). Their single-photon counting capability extends well beyond telecommunications wavelengths (up to 3 μm).[11]

In this paper we report the full characterization of single-photon source emitting at 902 nm using a pair of SSPDs, via spontaneous emission lifetime and $g^{(2)}(\tau)$ antibunching measurements. We demonstrate, via detailed analysis and measurements on an attenuated laser at 1550 nm, that the current twin SSPD detector scheme is well suited for the characterization of single-photon sources at telecommunications wavelengths (1310 and 1550 nm).

II. EXPERIMENT

A. Superconducting single-photon detector system

Each SSPD is based on a narrow superconducting track (100 nm wide, covering a 10×10 μm^2 area with a 50% fill factor) of NbN.[10,11] The photodetection mechanism is as follows: the superconducting track is biased close to its critical current. When the track absorbs a photon, a hotspot is formed, briefly creating a resistive region across the width of the track. The resultant voltage pulse can be amplified and measured. In our detector system, each device is aligned to optical fiber at room temperature using a microalignment stage under a long focal length microscope.[14] Due to the small area of the SSPDs (10×10 μm^2), the practical η of fiber-coupled SSPDs (Refs. 14 and 15) often falls significantly short of the best-reported intrinsic η values.[12,13] Using our alignment technique, we are now able to consistently achieve good fiber coupling ($\eta\sim1\%$ at low dark count rates) for all our SSPDs, which is essential in carrying out the experiment reported here.

The packaged devices are mounted in a commercial cryogen-free refrigerator, with base temperature of ~2.5 K.[14] The refrigerator has a sufficient cooling capacity (100 mW at 4 K) to accommodate four or more fiber-coupled detector channels. In this experiment we use two fiber-coupled SSPDs temperature stabilized at 3.1 K. Our detectors are biased with low-noise current sources with careful attention to grounding to eliminate spurious dark count events induced by electrical pickup and cross-talk. Furthermore we have used our timing electronics (see below) to investigate possible correlations between detection events on the two SSPD channels, both in terms of the dark counts on the two channels and in terms of photoinduced counts on one channel and dark counts on the other. We have found no evidence of electrical or optical cross-talk.

[a]Present address: School of Engineering and Physical Sciences, Heriot-Watt University, Edinburgh, EH14 4AS, United Kingdom; electronic mail: r.h.hadfield@hw.ac.uk

 © 2007 American Institute of Physics

Downloaded 31 May 2007 to 132.163.53.117. Redistribution subject to AIP license or copyright, see http://jap.aip.org/jap/copyright.jsp

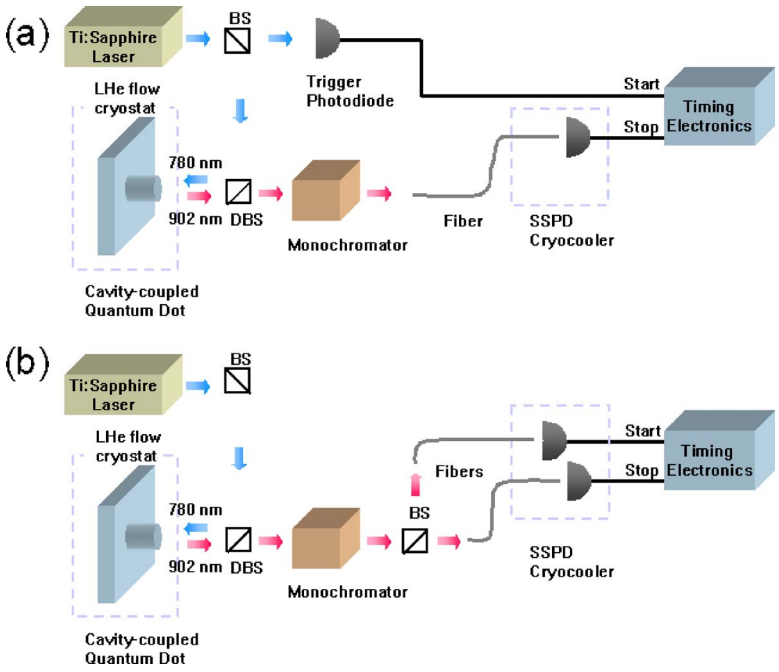

FIG. 1. (Color online) (a) Setup for spontaneous emission lifetime measurement on a quantum dot single-photon source. A fast photodiode is used as the start trigger for the timing electronics; the stop is provided by an SSPD. (b) Setup for $g^{(2)}(\tau)$ experiment. A standard Hanbury Brown–Twiss configuration is used with SSPDs at each output. SSPD—superconducting single-photon detector, BS—beamsplitter, and DBS—dichroic beam splitter.

B. Quantum dot single-photon source

The single-photon source is an individual InGaAs quantum dot embedded inside a micropillar cavity.[4,5] The optical cavity is formed by a pair of GaAs/AlAs distributed Bragg reflectors grown above and below the dot, and a cylindrical micropillar ~ 2 μm in diameter is defined with a reactive ion etch. The dot is optically pumped with a Ti:sapphire laser (~ 1 ps pulses, center wavelength $\lambda = 780$ nm, and 82 MHz repetition rate) and cooled to ~ 5 K in a liquid He flow cryostat. At this temperature, the dot is on resonance with the cavity and emits single photons at $\lambda = 902$ nm. The photoluminescence (PL) emitted from the micropillar is collected with an objective lens and directed through a monochromator. Single photons arrive at the output of the monochromator at a rate of ~ 100 kHz. The properties of the PL are studied using the setups depicted in Fig. 1. The PL photons are launched into the telecommunications fiber and hence coupled to the SSPDs.

C. Spontaneous emission lifetime measurement setup

The measurement configuration is based on the apparatus depicted in Fig 1(a).[16] For this measurement we used time-to-amplitude-converter/multichannel analyzer timing electronics with low jitter (below 30 ps). In this instance a fast photodiode triggered directly by the laser pulse starts the timing electronics, and a single SSPD triggered by the photoluminescence provides the stop. To measure the temporal instrument response function (IRF) of a detector, we tune the monochromator to 780 nm and heavily attenuate the beam, triggering the SSPD directly with photons from the laser.

D. $g^{(2)}(\tau)$ measurement setup

The measurement configuration is based on the apparatus depicted in Fig. 1(b). For the $g^{(2)}(\tau)$ antibunching measurement, PL from the source is directed into a free-space Hanbury Brown–Twiss (HBT) interferometer. The outputs of the HBT interferometer are coupled to the fiber inputs of a pair of SSPDs. The timing electronics used for this experiment has 160 ps full width at half maximum (FWHM) jitter. The η of each SSPD detection channel (inclusive of fiber coupling losses from free space into fiber and from fiber to detector) is $\sim 2\%$ at 902 nm. The count rate per channel was ~ 600 Hz, indicating that the mean photon number per clock cycle entering the HBT is $\mu = 7.5 \times 10^{-4}$. The dark count rate is extremely low (below 10 Hz per channel), giving P_{dark} per 0.55 ns bin of 5.5×10^{-9}.

III. SINGLE-PHOTON SOURCE CHARACTERIZATION

A. Spontaneous emission lifetime results at 902 nm

An important measure of the quality of a single-photon source is the spontaneous emission lifetime, which intrinsically limits the source jitter. When the dot is on resonance with the cavity, the PL lifetime will be shortened due to the Purcell effect. The PL lifetime and IRF data are shown in Fig. 2. The SSPD's response is fitted very well—over four decades of dynamic range—by a Gaussian with a FWHM of 68 ps. The Gaussian IRF of the SSPD makes it straightforward to deconvolve the spontaneous emission lifetime of the source—in this case 400 ps.

B. $g^{(2)}(\tau)$ measurement results at 902 nm

The crucial measure of the quality of a single-photon source is the second-order correlation function, $g^{(2)}(\tau)$. A suppressed multiphoton emission probability is indicated by $g^{(2)}(0) < 1$; a true single-photon source will have $g^{(2)}(0) = 0$. In the limit $\mu\eta \ll 1$, the histogram of counts versus the delay time τ, between start and stop triggers from the single-photon detectors at the outputs of the HBT interferometer, is proportional to $g^{(2)}(\tau)$. Figure 3 shows a measurement of $g^{(2)}(\tau)$, pumped at a clock frequency f of 82 MHz. The

Downloaded 31 May 2007 to 132.163.53.117. Redistribution subject to AIP license or copyright, see http://jap.aip.org/jap/copyright.jsp

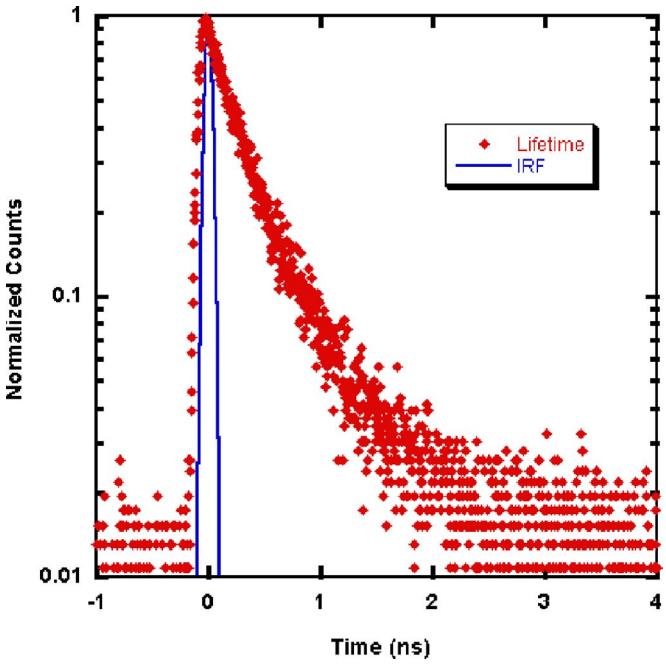

FIG. 2. (Color online) Spontaneous emission lifetime of a quantum dot measured with a single SSPD channel. The start clock to timing electronics is provided by a fast photodiode driven directly by the Ti: sapphire pump laser. The carrier lifetime of the source is ~400 ps. The instrument response function (IRF) of the SSPD is a 68 ps FWHM Gaussian.

counts are binned at 0.55 ns intervals. The counts in the histogram are accumulated across the full measurement window ($\Delta T = 16\ \mu s$) at a rate of ~6/s. The width of the peaks (~1.4 ns FWHM) is dominated by the jitter of the quantum dot single-photon source and the timing electronics. Owing to the exceptionally low dark count rates on the detectors, there are very few counts between peaks—even though the acquisition time was several hours. The area of each peak in the histogram is calculated by summing all the counts in a 3 ns time window. Dividing the area of the peak at $\tau = 0$ by the mean area of all other recorded peaks $\tau \neq 0$ in the measurement window, ΔT, yields a second-order intensity correlation $g^{(2)}(0) = 0.081 \pm 0.038$, indicating that the probability of two-photon emission from the source is extremely low.

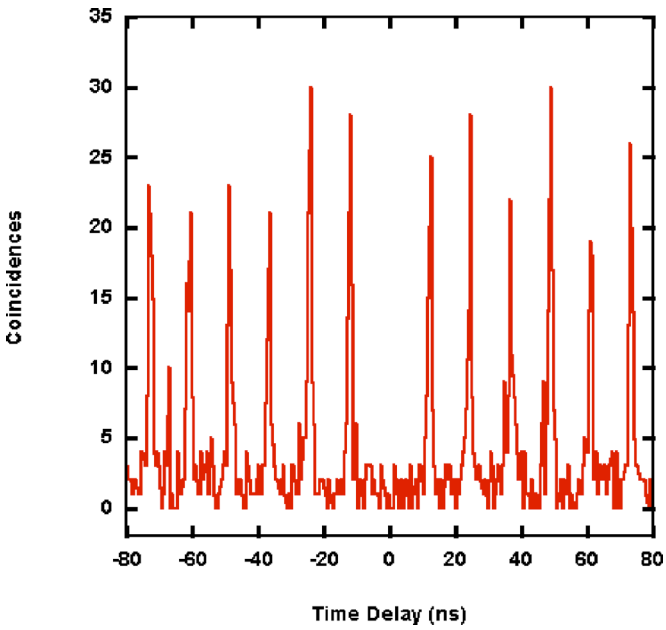

FIG. 3. (Color online) $g^{(2)}(\tau)$ for a cavity-coupled quantum dot using twin SSPDs. Data binned at 0.55 ns intervals. The SSPDs have a detection efficiency η (including fiber coupling losses) of 2% per channel. They are biased such that the dark count rate is ~10 Hz. The measured $g^{(2)}(0) = 0.081 \pm 0.038$.

C. Evaluation of detector performance in 902 nm $g^{(2)}(0)$ measurement

We have shown empirically that our twin SSPD setup can be used to provide a high fidelity characterization of a single-photon source at 902 nm. In this section we present a detailed analysis in order to compare performance of different detectors in the $g^{(2)}(\tau)$ experiment.

Our first goal in this analysis is to calculate the effect of measuring a source with $g^{(2)}(0) \ll 1$ with imperfect detectors. The raw measured $g^{(2)}(0)$ is the counts at zero delay N_0 divided by the average height of a peak at nonzero delay N_τ,

$$g_{\text{raw}} = \frac{N_0}{N_\tau}. \tag{1}$$

If there is a significant level of background counts per bin B, either due to stray light or detector dark counts, g_{raw} includes an offset. If B can be measured with good statistics, a more accurate measure of $g^{(2)}(0)$ for the source can be obtained by background subtraction,

$$g_{\text{corrected}} = \left(\frac{N_0 - B}{N_\tau - B} \right). \tag{2}$$

In order to provide a self-consistency check in our measurement of $g^{(2)}(0)$ on the source at 902 nm and to provide a means of comparing the detectors, we evaluate (1) in terms of the detector properties (η and P_{dark}). Assuming an ideal 50:50 beamsplitter, the probability of a single detection event on either channel per clock cycle (providing either a "start" or a "stop" trigger to the timer) is $\frac{1}{2}\mu\eta$, where μ is the mean photon number per clock cycle entering the HBT. The probability of source-triggered counts per clock cycle at $\tau \neq 0$, S, is given by

$$S = \frac{1}{4}\mu^2\eta^2. \tag{3}$$

The probability of a count with an accidental start or stop trigger per clock cycle A is given by

$$A = \left(\frac{1}{2}\mu\eta + P_{\text{back}} \right)^2 - \frac{1}{4}\mu^2\eta^2, \tag{4}$$

where P_{back} includes the dark count probability P_{dark} and background light triggered events. Thus for a perfect single-photon source [$g^{(2)}(0) = 0$], the offset to the measured value of $g^{(2)}(0)$ is

$$g_{\text{offset}} = \frac{B}{N_\tau} = \frac{A}{A+S} = \frac{1}{1+S/A}, \tag{5}$$

and

Downloaded 31 May 2007 to 132.163.53.117. Redistribution subject to AIP license or copyright, see http://jap.aip.org/jap/copyright.jsp

TABLE I. Comparison of single-photon counting detectors for $g^{(2)}(\tau)$ measurements on single-photon sources. The dark count probability P_{dark} is calculated per nanosecond. g_{offset} is the offset in the measured value of $g^{(2)}(0)$ in the limit where all background counts are due to dark counts. The time for pattern to emerge is calculated with the same experimental statistics calculated with ten source-triggered counts per $\tau \neq 0$ cycle, at a mean photon number per pulse entering the Hanbury Brown–Twiss of $\mu = 7.5 \times 10^{-4}$.

Detector	Si APD	SSPD	InGaAs APD[a]	SSPD		New SSPD[b]
Detection efficiency, η	0.38	0.02	0.05	0.02		0.57
λ (nm)	902	902	1300	1550		1550
Dark count rate, R_{dark} (Hz)	100	10	3×10^4	1000		⋯
Dark count probability, P_{dark} $(\mathrm{ns})^{-1}$	10^{-7}	10^{-8}	3×10^{-5}	10^{-6}		⋯
g_{offset} (3 ns bin)	0.0042	0.0080	0.97	0.49		⋯
g_{offset} (300 ps bin)	0.0004	0.0008	0.54	0.075		⋯
Frequency, f (MHz)	82	82	4	82	1000	82
Accumulation rate per cycle $=(\frac{1}{2}\mu\eta)^2 f$ (Hz)	1.6	0.0046	0.0014	0.0046	0.056	3.74
Time for pattern to emerge (s)	6	2200	7100	2200	180	2.7
Time taken to obtain $\sigma\,(g_{\mathrm{corrected}}) = 0.05$ (300 ps bin) (s)	⋯	⋯	3.4×10^5	7100	580	⋯

[a]For the InGaAs APD, η, R_{dark}, and the minimum bin size are quoted/deduced from. Ref. 18. Other values for the InGaAs APD are calculated using a μ of 7.5×10^{-4} per clock cycle (from our current 902 nm experiment) for ease of comparison with other detectors. In Ref. 18 a higher μ was achieved, and the duration of the experiment was longer, leading to a lower $g^{(2)}(0)_{\mathrm{offset}}$, lower uncertainties, and faster accumulation rate than the values given in this table.
[b]The entries for the final column are incomplete as the dark count rate is not given in Ref. 21.

$$\frac{S}{A} = \frac{\mu^2\eta^2}{4(\mu\eta P_{\mathrm{back}} + P_{\mathrm{back}}^2)} \simeq \frac{\mu\eta}{4P_{\mathrm{dark}}}. \tag{6}$$

The approximation holds if background light sources are effectively excluded in the experiment such that $P_{\mathrm{back}} \rightarrow P_{\mathrm{dark}}$ and $P_{\mathrm{dark}} \ll \mu\eta$. Therefore the ratio η/P_{dark} (at a given μ) sets a lower limit on g_{raw}, and is thus a suitable metric for comparing detector performance. This result can be found (in a somewhat different form) elsewhere;[17] our intention here is to set out the analysis clearly in terms of the detector properties (η, P_{dark}) to allow comparison between different detector types.

Using Eqs. (5) and (6) we can critically evaluate the performance of our SSPD detector system in the 902 nm single-photon source experiment. Table I illustrates the results of the analysis. Relative to a commercially available Si APD ($\eta = 0.38$, dark count rate of 100 Hz) the SSPD ($\eta = 0.02$, dark count rate of 10 Hz) has a comparable signal to noise—thus we expect a $g^{(2)}(0)$ measurement of excellent fidelity in both cases; with no source of background counts other than detector dark counts we expect $g_{\mathrm{offset}} \sim 10^{-3}$. In our actual measurement $g^{(2)}(0)$ determined from g_{raw} was 0.081 with an uncertainty of 0.038. In our experiment $P_{\mathrm{back}} \gg P_{\mathrm{dark}}$, i.e., background counts due to stray light or spurious events recorded by the timing electronics dominated over actual detector dark counts. By blocking the optical input of one of the detectors, we found that spurious start or stop triggers led to false counts being recorded by the timing electronics, an order of magnitude in excess of rate expected from the measured dark count rate on the optically blocked channel. Nevertheless, as is evident from the actual measurement of $g^{(2)}(\tau)$ in Fig. 3, there is still less than one background count per 0.55 ns time bin in the histogram, so the uncertainty in B is still too large to consider background subtraction.

A further important practical consideration for a tractable experiment is the accumulation rate of source-triggered start-stop counts in the histogram per $\tau \neq 0$ cycle,

$$R = Sf = \left(\frac{1}{2}\mu\eta\right)^2 f = \frac{1}{4}\mu^2\eta^2 f. \tag{7}$$

Hence, in the limit $S \gg A$, detectors with high η and fast recovery times are preferable. The acquisition time can be estimated from Eq. (7). For a 902 nm $g^{(2)}(\tau)$ experiment, both SSPD and Si APD detectors can be used (in the limit $\eta\mu \ll 1$) with a source pumped at 82 MHz, so the estimated acquisition time is much slower for the SSPD due to reduced η. An estimate is given in Table I of the time for the $g^{(2)}(\tau)$ pattern to emerge (>10 source-triggered counts per clock cycle at $\tau \neq 0$, mean photon number per pulse $\mu = 7.5 \times 10^{-4}$).

D. Towards single-photon source characterization at telecommunications wavelengths

Now let us use the equations derived above to evaluate the detector performance in a $g^{(2)}(\tau)$ measurement on a single-photon source at telecommunications wavelengths, and to demonstrate not only that such a measurement is feasible with our current twin SSPD system but also that a

Downloaded 31 May 2007 to 132.163.53.117. Redistribution subject to AIP license or copyright, see http://jap.aip.org/jap/copyright.jsp

measurement of superior quality can be made. Results of the analysis are again shown in Table I. In previous studies, single-photon sources emitting near 1.3 μm have been characterized with InGaAs APDs.[6,18] However, the strong probability of afterpulsing and high dark count rates in these detectors make low laser repetition rates (2–4 MHz) and temporal gating of the InGaAs APDs essential. In order to improve the ratio η/P_{dark}, each detector is active for as little as 300 ps once every 250 ns.[18] In this mode the InGaAs APD η is reduced to ~0.05 (deduced from Ref. 18). The high background count rate means that $g^{(2)}(0)$ as determined from g_{raw} will contain a significant g_{offset}. In Table I (assuming $\mu=7.5\times10^{-4}$) we see that even for a 300 ps bin, g_{offset} is 0.54. Ideally one would subtract the background B to determine the actual value of $g^{(2)}(0)$ for the single-photon source. However, in practice using the InGaAs APDs, B is difficult to measure independently, since the resulting histograms record only one time bin per laser pulse.[6,18] Later in this section we show that even if the B can be well determined, background subtraction on a histogram acquired using detectors with poor η/P_{dark}, such as InGaAs APDs, introduces a large uncertainty in the estimate of $g^{(2)}(0)$.

The twin SSPD system detailed here could be used to characterize a source at 1310 or 1550 nm without the problems afflicting InGaAs APDs, and should yield a result qualitatively similar to the histogram shown in Fig. 3, where data are collected into a continuous band of time bins that covers the entire range during and between laser pulses. At 1550 nm, $\eta\sim0.02$ per channel is achievable at the expense of elevated dark counts (~1 kHz). For a given bin width and mean photon number per pulse μ, we can anticipate a lower g_{offset} for the SSPD as η/P_{dark} is higher and background counts accumulate at a lower rate—in Table I we see (for the same μ) at 300 ps bin width, g_{offset} is 0.075. According to Eq. (7) the improved clock frequency of the SSPD (82 MHz) will easily compensate for the reduction of η and lead to shortened acquisition time. It is salient to note that as the SSPD does not need to be gated, and has a short recovery time (below 10 ns),[19] it can in principle be operated with a continuous wave (cw) pumped source.[20] The internal dynamics of the source will probably limit the effective clock rate to ~1 GHz. As shown in Table I, for a clock rate of 1 GHz the accumulation rate is dramatically increased. A further point to note is that SSPD designs have been reported with intrinsic η up to 57%.[21] If the η of these detectors can be exploited by efficient optical coupling, the efficiency of the $g^{(2)}(\tau)$ experiment will be greatly improved, to the level expected from Si APDs on single-photon sources emitting below 1000 nm.

In order to provide a full comparison between detector types [particularly in the telecommunication wavelength $g^{(2)}(\tau)$ measurement], it is insightful to extend the analysis of the previous section to consider the uncertainty both in g_{raw} and in the estimate of the value of $g^{(2)}(0)$ from $g_{\mathrm{corrected}}$ obtained via background subtraction. The main results are shown here; a full derivation is given in the Appendix.

To evaluate whether background subtraction will lead to an improved determination of $g^{(2)}(0)$, firstly consider the uncertainty in g_{raw}, for an experiment of duration $T_{\mathrm{experiment}}$, in the limit where the source $g^{(2)}(0)=0$,

$$\frac{\sigma(g_{\mathrm{raw}})}{g_{\mathrm{raw}}} \simeq \left(\frac{1}{N_0}+\frac{1}{N_\tau}\right)^{1/2} = \left\{\left(\frac{1}{AT_{\mathrm{experiment}}f}\right)+\left[\frac{1}{(S+A)T_{\mathrm{experiment}}f}\right]\right\}^{1/2}. \quad (8)$$

For a detector with poor η/P_{dark} (such as the InGaAs APD), g_{offset} will be large. However, we may be able to obtain good statistics on g_{raw} for a reasonable $T_{\mathrm{experiment}}$, so background subtraction is a strategy worth considering to obtain a better estimate of the source $g^{(2)}(0)$. The measurements at 902 nm with Si APDs and SSPD (see above and Ref. 14) are in the limit $S\gg A$, thus g_{offset} will be small and the fractional uncertainty in g_{raw} becomes $(N_0)^{-1/2}\simeq(B)^{-1/2}=(AT_{\mathrm{experiment}}f)^{-1/2}$. In this limit, unless $T_{\mathrm{experiment}}$ is long (such that the average number of background counts per bin $B>1$) and $g^{(2)}(0)$ is smaller even than g_{offset}, there is little to be gained from background subtraction.

Let us now consider how uncertainties propagate when the background counts B are subtracted. The value of $g^{(2)}(0)$ determined by background subtraction is given by Eq. (2). In the limit $g^{(2)}(0)\ll1$, $N_0\approx B$; assuming B can be measured to high precision, we find

$$\sigma(g_{\mathrm{corrected}}) \simeq \frac{(\eta\mu P_{\mathrm{dark}}+P_{\mathrm{dark}}^2)^{1/2}}{[(1/2)\mu\eta]^2(T_{\mathrm{experiment}}f)^{1/2}}. \quad (9)$$

In Table I we calculate how long we need to measure to achieve a 5% uncertainty in $g_{\mathrm{corrected}}$ (again assuming $\mu=7.5\times10^{-4}$). Viewed from this perspective, the differences between the detectors are thrown into sharp relief. For the SSPD clocked at 82 MHz this level of uncertainty will be obtained in 7100 s (~2 h); for the InGaAs APD, even if B can be determined with good accuracy, the experiment will take 3.4×10^5 s (~100 h). For the SSPD with cw pump (1 GHz) this level of accuracy will be obtained in 580 s (less than 10 min). Again we emphasize that any improvement in the experimental μ will reduce this time for either detector.

As a final demonstration, since we do not currently have a single-photon source in the 1300–1550 nm range available, we have instead used our system to perform a $g^{(2)}(\tau)$ measurement on a pulsed laser at 1550 nm (Fig. 4). The data are binned at 0.55 ns intervals. The 1550 nm laser is gain switched by voltage pulses from a signal generator at 79 MHz. The mean detected photon number per pulse ($\mu\eta$) in this measurement is 8.4×10^{-4}. The histogram of counts versus time delay is thus proportional to $g^{(2)}(\tau)$ for the source. As expected for a Poissonian source the peak at zero time delay remains and $g^{(2)}(0)=1$. The breadth of the peaks in the histogram (3.3 ns FWHM) is due to the relatively long pulse length of the source (2.3 ns).

IV. CONCLUSIONS

We report on the performance of a superconducting single-photon detector system for characterizing single-

Downloaded 31 May 2007 to 132.163.53.117. Redistribution subject to AIP license or copyright, see http://jap.aip.org/jap/copyright.jsp

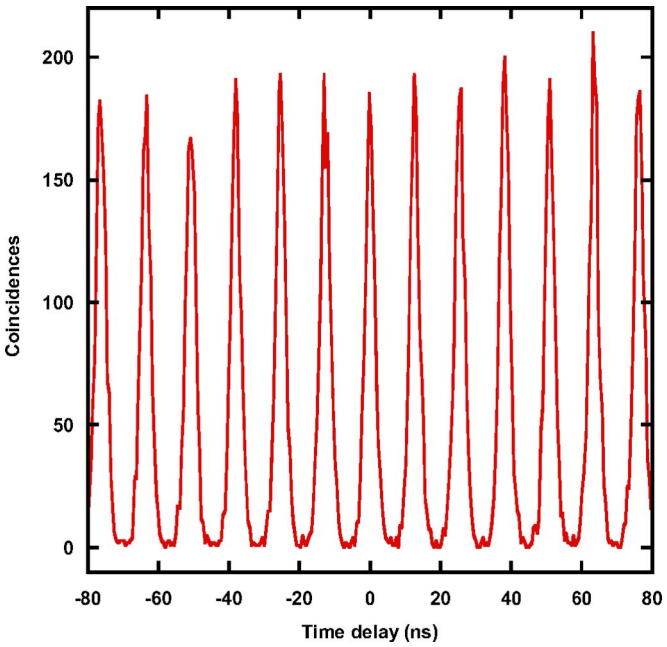

FIG. 4. (Color online) $g^{(2)}(\tau)$ of a 1550 nm diode laser gain switched at 1550 nm measured with twin SSPDs. As expected for a Poissonian source, $g^{(2)}(0)=1$. The width (3.3 ns FWHM) of the peaks is dominated by the jitter (2.3 ns FWHM) of the laser.

photon sources. Our two detector channels are housed within the same cryogen-free refrigerator with no evidence of electrical or optical cross-talk. At 902 nm, the detection efficiency η of our detector system is 2% per channel, inclusive of coupling losses. The low jitter (68 ps FWHM with Gaussian profile) and low dark counts (10 Hz per channel) of the detector allow a spontaneous emission lifetime measurement of high accuracy to be carried out on the source. We also obtain a $g^{(2)}(\tau)$ measurement of excellent fidelity on a single-photon source at 902 nm using twin SSPDs $[g^{(2)}(0)=0.081\pm0.038]$. Moreover, via detailed analysis and measurements on a Poissonian source at 1550 nm, we have demonstrated that this detector system can be employed for $g^{(2)}(\tau)$ measurements on single-photon sources at telecommunications wavelengths and offers significant advantages over InGaAs APDs.

In addition to the $g^{(2)}(\tau)$ measurement discussed here, the SSPD detector system will enable a host of other advances in the realm of quantum information processing. These detectors will enable the further studies of quantum emitters, in particular time correlations between different emission lines of the same dot. The SSPD detector system has recently been used in quantum key distribution demonstrations at 1550 nm[22] and 850 nm[23] wavelengths and in measurements on 1550 nm photon pairs.[20,24] This detector technology should enable quantum state tomography of entangled photons at 1550 nm. Improvements in detector performance are anticipated: with further investment in low noise electronics or improved device design we anticipate an improvement in jitter. Similarly, device designs incorporating the detector in an optical cavity may facilitate a considerable boost in available η in the near future.[21]

ACKNOWLEDGMENTS

This work was carried out with the support of the DARPA QuIST program, the DTO, the NIST Quantum Information Science Initiative, and the U.S. Department of Commerce. We thank N. Bergren and R. Schwall for technical assistance and G. Gol'tsman for providing the detectors used in this work.

APPENDIX: DERIVATION OF UNCERTAINTIES

Let N_0 be the number of the counts in the clock cycle at zero time delay ($\tau=0$) and N_τ be the (mean) number of counts in a cycle at nonzero time delay ($\tau\neq0$). B is the number of background counts per bin in the histogram. $T_{\text{experiment}}$ is the duration of the experiment. Measured value of $g^{(2)}(0)$,

$$g_{\text{raw}}=\frac{N_0}{N_\tau}. \tag{A1}$$

The uncertainty in the measured value of $g^{(2)}(0)$ (where the actual value of $g^{(2)}(0)=0$) is

$$\begin{aligned}\frac{\sigma(g_{\text{raw}})}{g_{\text{raw}}} &\simeq \left[\left(\frac{\sigma_{N_0}}{N_0}\right)^2+\left(\frac{\sigma_{N_\tau}}{N_\tau}\right)^2\right]^{1/2}\\ &\simeq \left[\left(\frac{1}{N_0}\right)+\left(\frac{1}{N_\tau}\right)\right]^{1/2} \quad (\sigma_{N_i}\simeq\sqrt{N_i})\\ &= \left\{\left(\frac{1}{AT_{\text{experiment}}f}\right)\right.\\ &\quad \left.+\left[\frac{1}{(S+A)T_{\text{experiment}}f}\right]\right\}^{1/2} \quad (N_0=B)\\ &\simeq \left(\frac{1}{AT_{\text{experiment}}f}\right)^{1/2} \quad (S\gg A)\end{aligned} \tag{A2}$$

Value of $g^{(2)}(0)$ determined by background subtraction,

$$g_{\text{corrected}}=\left(\frac{N_0-B}{N_\tau-B}\right). \tag{A3}$$

Uncertainty in determination of $g^{(2)}(0)$ (assuming N_0, B, and N_τ are independent),

$$\begin{aligned}\sigma(g_{\text{corrected}})^2 &\simeq \left(\frac{\partial g_{\text{corrected}}}{\partial N_0}\right)^2\sigma_{N_0}^2+\left(\frac{\partial g_{\text{corrected}}}{\partial B}\right)^2\sigma_B^2\\ &\quad +\left(\frac{\partial g_{\text{corrected}}}{\partial N_\tau}\right)^2\sigma_{N_\tau}^2\\ &= \left[\frac{1}{(N_\tau-B)}\right]^2\sigma_{N_0}^2+\left[\frac{1}{(N_\tau-B)}\right.\\ &\quad \left.-\frac{(N_0-B)}{(N_\tau-B)^2}\right]^2\sigma_B^2+\left[\frac{(N_0-B)}{(N_\tau-B)^2}\right]^2\sigma_{N_\tau}^2.\end{aligned} \tag{A4}$$

In the limit $g^{(2)}(0)\ll1$, $N_0\approx B$. Hence,

Downloaded 31 May 2007 to 132.163.53.117. Redistribution subject to AIP license or copyright, see http://jap.aip.org/jap/copyright.jsp

$$\sigma(g_{\text{corrected}})^2 \simeq \left[\frac{1}{(N_\tau - B)}\right]^2 \sigma_{N_0}^2 + \left[\frac{1}{(N_\tau - B)}\right]^2 \sigma_B^2. \quad \text{(A5)}$$

Furthermore if the background B can be measured with good precision, σ_B can be minimized.

$$\sigma(g_{\text{corrected}})^2 \simeq \left[\frac{1}{(N_\tau - B)}\right]^2 \sigma_{N_0}^2 \simeq \left[\frac{1}{(N_\tau - B)}\right]^2 N_0 \quad (\sigma_{N_0} \simeq \sqrt{N_0}), \quad \text{(A6)}$$

$$\therefore \sigma(g_{\text{corrected}})^2 \simeq \frac{AT_{\text{exp}}f}{S^2 T_{\text{exp}}^2 f^2} = \frac{A}{S^2 T_{\text{exp}} f}, \quad \text{(A7)}$$

$$\therefore \sigma(g_{\text{corrected}}) \simeq \frac{(\eta\mu P_{\text{dark}} + P_{\text{dark}}^2)^{1/2}}{\left(\frac{1}{2}\mu\eta\right)^2 (T_{Exp} f)^{1/2}}. \quad \text{(A8)}$$

[1] C. H. Bennett and G. Brassard, *Proceedings of IEEE International Conference on Computers, Systems and Signal Processing*, Bangalore, India (IEEE, New York, 1984), pp. 175–179.
[2] N. Gisin, G. Ribordy, W. Tittel, and H. Zbinden, Rev. Mod. Phys. **74**, 145 (2002).
[3] E. Knill, R. Laflamme, and G. J. Milburn, Nature (London) **409**, 46 (2001).
[4] P. Michler, A. Kiraz, C. Becher, W. V. Schoenfeld, P. M. Petroff, L. D. Zhang, E. Hu, and A. Imamoglu, Science **290**, 2282 (2000).
[5] C. Santori, M. Pelton, G. Solomon, Y. Dale, and Y. Yamamoto, Phys. Rev. Lett. **86**, 1502 (2001).
[6] M. B. Ward *et al.*, Appl. Phys. Lett. **86**, 201111 (2005).
[7] B. Alloing *et al.*, Appl. Phys. Lett. **86**, 101908 (2005).
[8] T. E. Ingerson, R. J. Kearney, and R. L. Coulter, Appl. Opt. **22**, 2013 (1983).
[9] F. Zappa, A. Lacaita, S. Cova, and P. Webb, Opt. Lett. **19**, 846 (1994).
[10] G. N. Gol'tsman *et al.*, Appl. Phys. Lett. **79**, 705 (2001).
[11] A. Verevkin *et al.*, Appl. Phys. Lett. **80**, 4687 (2002).
[12] A. Korneev *et al.*, Appl. Phys. Lett. **84**, 5338 (2004).
[13] A. Verevkin *et al.*, J. Mod. Opt. **51**, 1447 (2004).
[14] R. H. Hadfield, M. J. Stevens, S. G. Gruber, A. J. Miller, R. E. Schwall, R. P. Mirin, and S. W. Nam, Opt. Express **13**, 10846 (2005).
[15] W. Slyz *et al.*, Appl. Phys. Lett. **88**, 261113 (2006).
[16] M. J. Stevens, R. H. Hadfield, R. E. Schwall, S. W. Nam, R. P. Mirin, and J. A. Gupta, Appl. Phys. Lett. **89**, 031109 (2006). In this paper we report measurements on semiconductor samples emitting at wavelengths up to 1245 nm; we have recently characterized samples emitting at 1650 nm.
[17] R. Brouri, A. Beveratos, J.-P. Poizat, and P. Grangier, Opt. Lett. **25**, 1294 (2000).
[18] C. Zinoni *et al.*, Appl. Phys. Lett. **88**, 131102 (2006).
[19] R. H. Hadfield, A. J. Miller, S. W. Nam, R. L. Kautz, and R. E. Schwall, Appl. Phys. Lett. **87**, 203505 (2005).
[20] M. J. Jaspan, J. Habif, R. H. Hadfield, and S. W. Nam, Appl. Phys. Lett. **89**, 031112 (2006).
[21] K. M. Rosfjord, J. K. W. Yang, E. A. Dauler, A. J. Kerman, V. Anant, B. M. Voronov, G. N. Gol'tsman, and K. K. Berggren, Opt. Express **14**, 527 (2006).
[22] R. H. Hadfield, J. L. Habif, J. Schlafer, R. E. Schwall, and S. W. Nam, Appl. Phys. Lett. **89**, 241129 (2006).
[23] R. J. Collins, R. H. Hadfield, V. Fernandez, S. W. Nam, and G. S. Buller, Electron. Lett. **43**, 180 (2007).
[24] C. Liang, K. F. Lee, M. Medic, P. Kumar, R. H. Hadfield, and S. W. Nam, Opt. Express **1**, 1322 (2007).

Downloaded 31 May 2007 to 132.163.53.117. Redistribution subject to AIP license or copyright, see http://jap.aip.org/jap/copyright.jsp